[Invited Tutorial Review Article Submitted to *Chemical Society Reviews*]

Controlled Growth of Single-Walled Carbon Nanotubes on Patterned Substrates

Xiaozhu Zhou,[1] Freddy Boey,[1,2] Hua Zhang[*,1,2]

[1]School of Materials Science and Engineering, Nanyang Technological University, 50 Nanyang Avenue, Singapore 639798, Singapore.

[2]Centre for Biomimetic Sensor Science, Nanyang Technological University, 50 Nanyang Drive, Singapore 637553, Singapore.

*Corresponding author. E-mail: hzhang@ntu.edu.sg, hzhang166@yahoo.com

Website: http://www.ntu.edu.sg/home/hzhang/

Abstract

Single-walled carbon nanotubes (SWCNTs) have attracted great interest in the last two decades because of their unique electrical, optical, thermal, mechanical properties, *etc.* One major research field of SWCNTs is the controlled growth of them from the patterned catalysts on substrates, since the integration of SWCNTs into nanoelectronics and other devices requires well-organized SWCNT arrays. This tutorial review describes the commonly used lithographic techniques to pattern catalysts used for controlled growth of SWCNTs, specifically confined to horizontal direction. Advantages and disadvantages of each method will be briefly discussed. Applications of the SWCNT arrays grown from the catalyst patterns will also be introduced.

1. Introduction

Since the observation of multi-walled carbon nanotubes (CNTs) by Iijima in 1991,[1] tremendous progress has been made in the research of CNTs in the last two decades. CNT is a family of quasi one-dimensional tubular structure, which can form by rolling up graphene sheet(s) made up of single layer of sp^2 carbon atoms that are densely packed in a honeycomb lattice structure.[2] Depending on the layer number of graphene sheets, single-walled or multi-walled CNTs can be resulted. Among them, single-walled CNTs (SWCNTs)[3] have attracted the most intense interest because of their excellent electrical (carrier mobility as high as 100,000 $cm^2V^{-1}s^{-1}$), mechanical (Young's modulus of 1 TPa and tensile strength of 30 GPa), thermal (6,600 $Wm^{-1}K^{-1}$ at room temperature), optical, and sensing properties.[4] Besides, the graphene structure renders SWCNTs exceptional chemical stability. All these properties make SWCNTs promising candidates in many applications, such as composites, electronics, and optoelectronics, *etc*.[5] Among them, because of the small size and superb electrical property, SWCNTs have been touted as alternative building blocks for future nanoelectronics to replace the current silicon. This is because the dimension of silicon-based electronic circuits has reached its limits governed by the current technology and fundamental physics (quantum effect).[6] However, in order to apply SWCNTs in electronics and other classes of devices, it is critically important to assemble SWCNTs into arrays which are crucial for their integration to devices. In particular, it is desirable to obtain SWCNT arrays with defined locations and directions, and controlled density. For example, parallel alignment of SWCNTs is important to avoid the tube-tube junctions, which can limit the effective transport in the SWCNT thin film and cause junction barriers.[7] To date, two major strategies have been employed to achieve the assembly of SWCNTs. One is to grow and assemble SWCNTs selectively on catalytically patterned substrates. The other is to post-

assemble SWCNTs from their suspensions.[8] Because the post-assembly method requires the treatment of SWCNTs (*e.g.* acid oxidation[9] and surfactant wrapping[10]) and thus lead to the destruction of their intrinsic properties (*e.g.* introduction of defects and shortening of length), much effort is made on the growth of SWCNTs on catalytically patterned substrates. It is worthy of notice that chemical vapor deposition (CVD) is the only method compatible with the growth of SWCNTs from the patterned catalysts on substrates. Therefore, the growth method in this review is CVD, instead of laser ablation and arc discharge which normally are used for substrate-free, bulk synthesis of SWCNTs with many byproduct impurities. The advantages of controlled growth of SWCNTs lie in not only that the intrinsic properties of SWCNTs are preserved, but also that the density, orientation and chirality of thus-grown SWCNTs are tunable. First, density and orientation control is important for their applications in electronics. For example, individual tube devices have been fabricated for gas sensors, exhibiting a fast response and high sensitivity.[11] Also, high performance electronics were demonstrated on dense, aligned SWCNTs.[12] Second, SWCNTs, behaving as metallic, semiconducting, or semi-metallic materials, are dependent on two key structural parameters, chirality and diameter, which in turn are determined by catalyst and CVD growth conditions. The optimization of catalysts (*i.e.* composition and size) and growth conditions have been widely studied on the bulk synthesis of SWCNTs.

Nevertheless, in order to gain all the advantages, one of the prerequisites is to pattern catalysts on substrates with a controlled manner. This review aims to introduce the various techniques to pattern catalysts for controlled growth of SWCNTs, ranging from conventional micro- and nanopatterning to non-conventional patterning techniques with brief illustrations of the advantages and disadvantages of each method.

The outline of this tutorial review is listed as follows. Section 2 introduces the important micropatterning and nanopatterning methods for generation of catalyst patterns to grow SWCNTs. Specifically, the commonly-used micropatterning techniques are illustrated in Section 2.1 (photolithography) and Section 2.2 (contact printing). A few typical nanolithographic methods are described in Section 2.3 (e-beam lithography and focused ion beam lithography) and Section 2.4 (dip-pen nanolithography). The "scratching" method, used for large-scale patterning of catalyst for growth of SWCNTs, is presented in Section 2.5. Other patterning methods are also briefly discussed in Section 2.6, including ink-jet printing, nanosphere lithography and block copolymer lithography. In Section 3, a particular example, *i.e.* SWCNT arrays are used as nanoantennas, is selected to illustrate the vast potential application of the grown SWCNT array. Last, in Section 4, we give a short summary and outlook of research challenges and opportunities that could advance the growth and applications of SWCNT arrays. Here, it is worth noting that in order to realize all the potential applications of grown SWCNT arrays in nanoelectronics and other areas, future research efforts should be focused on the control of chirality, density and grown direction of SWCNTs and their integration to devices.

2. Catalyst patterning techniques for growth of SWCNTs

2.1 Photolithography

Photolithography is a workhorse microfabrication technique and widely used in microelectronics. Due to its capability to pattern over large area, photolithography shows promises to pattern catalysts and thus the growth of SWCNT arrays on a wafer-scale which will render possible large-scale SWCNT devices, such as digital integrated circuits. For example, Dai *et al.* used the

deep ultraviolet (DUV) photolithography to pattern Fe/Mo catalysts on full 4-in. SiO_2/Si wafers.[13] In brief, a SiO_2/Si wafer was first coated with 300 nm thick of poly(methyl methacrylate) (PMMA) and exposed through a quartz mask to DUV. Large well structures were resulted in PMMA film upon developing the DUV-exposed regions, which would be filled with catalysts after spin-casting Al_2O_3 supported Fe/Mo catalysts on them. Upon baking the substrate at 160 °C for 5 min, the remaining PMMA regions was lifted off by immersion of the substrate in a dichloroethane, which afforded catalyst patterns with remarkable uniformity. Careful control of the experimental conditions in CVD, such as the feeding gas(es) and flow rate, is vital to the successful growth of SWCNTs. For example, when CVD is performed at 900 °C with CH_4 as the feeding gas, H_2 flow with only a certain flow rate leads to the growth of SWCNTs (100-150 mL min^{-1}). Whereas other flow rates of H_2 will lead to pyrolysis or inactive regimes. Meanwhile, the growth temperature dependence on H_2 flow rate was also identified. For example, since the reactivity of methane is higher at an elevated temperature (950 *vs.* 900 °C), a higher concentration of H_2 (200 *vs.* 125 mL min^{-1}) is required to inhibit CH_4 decomposition and bring the system into nanotube growth regime. The scale-up growth of SWCNTs on wafer scales described in this work makes it possible to integrate SWCNTs into nanoelectronics. However, thus-synthesized SWCNT arrays grow in random direction and also suffer from low density (less than 5 tubes μm^{-1}), inhibiting their adoption in real nanoelectronics wherein the alignment and high density of SWCNTs is imperative. Therefore, control of the alignment and density of CWCNTs is needed.

Although some strategies, such as gas flow[14] and external electric field,[15] can somewhat manipulate the orientation of SWCNTs during the growth process, the alignment of SWCNTs is not perfect. To date, the growth of perfectly-aligned and high density SWCNT arrays can be

achieved by growing them on substrates containing guiding crystal lattices. For example, when the catalyst lines are oriented perpendicular to the crystallographic lattice [110] on stable temperature (ST)-cut quartz substrates, CVD growth will yield SWCNT arrays with high levels of perfection aligned along [100]. Moreover, by increasing the density of the patterned catalysts, the density of SWCNTs can be increased. Rogers *et al.* have recently demonstrated high-performance electronics using dense, perfectly aligned arrays of SWCNTs, which were grown from patterned Fe lines.[12] Briefly, the patterning of Fe catalysts involved conventional photolithography to generate lines on photoresist (ZA 5214), followed by evaporation of Fe to nominal thickness of less than 0.5 nm. Lifting off the photoresist and annealing the Fe lines at 550 °C in air formed isolated iron oxide nanoparticles with a diameter of ~1 nm, which served as catalytic seeds for CVD growth of SWCNTs. Similar to Dai's work,[13] by control of the experimental conditions of CVD, *i.e.* purging with H_2 at 900 °C for 5 min and then introducing a flow of CH_4 (1900 sccm) and H_2 (300 sccm) at 900 °C for 1 h, the SWCNT arrays were obtained.[12] A density as high as 10 SWCNTs μm^{-1} was achieved. Figure 1A shows a scanning electron microscope (SEM) image of a pattern of perfectly aligned, perfectly linear SWCNTs. The high density and perfect alignment of SWCNTs allow one to integrate them into transistors. For example, the mobilities and scaled transconductances approaching ~1000 $cm^2V^{-1}s^{-1}$ and ~3000 Sm^{-1}, respectively, were reached when measurements were carried out on p- and n-channel transistors that involved as many as ~2100 SWCNTs. A current output of ~1 A is feasible in devices that use interdigitated electrodes. Besides, since it is practical to eliminate the metallic tubes from the SWCNT arrays using electrical breakdown,[16] the SWCNT arrays composed of almost semi-conducting tubes can be resulted, giving rise to better device performance, such as higher on/off ratio up to 10^5. Moreover, mechanically flexible transistors

on plastics (*e.g.* polyethylene terephthalate, PET) were also demonstrated after print transfer of aligned SWCNTs from quartz to PET. A recent study also by Rogers *et al.* demonstrated that the density in thus-aligned SWCNT arrays can be improved.[17] Their approach relies on multiple, separate CVD growth cycles on a single substrate. In brief, the first cycle of CVD was performed on catalyst lines with optimal densities of catalyst particles and separation between lines. Next, an additional set of catalyst lines was deposited in regions next to the original ones. SWCNTs would grow from the new catalyst lines for another cycle of CVD growth. Thus, the density of SWCNTs will increase (maybe double). For example, the density after the second growth can increase to a value of 7-15 SWCNT μm^{-1} from 4-7 SWCNT μm^{-1} of the first growth. From current-voltage (I-V) characteristics, the current levels measured from devices with double-growth SWCNTs are between 1.5 and 2 times larger than the single growth case. In principle, this method can be extended to triple or quadruple cycles or more, which could potentially realize densities approaching 100 SWCNTs μm^{-1}.

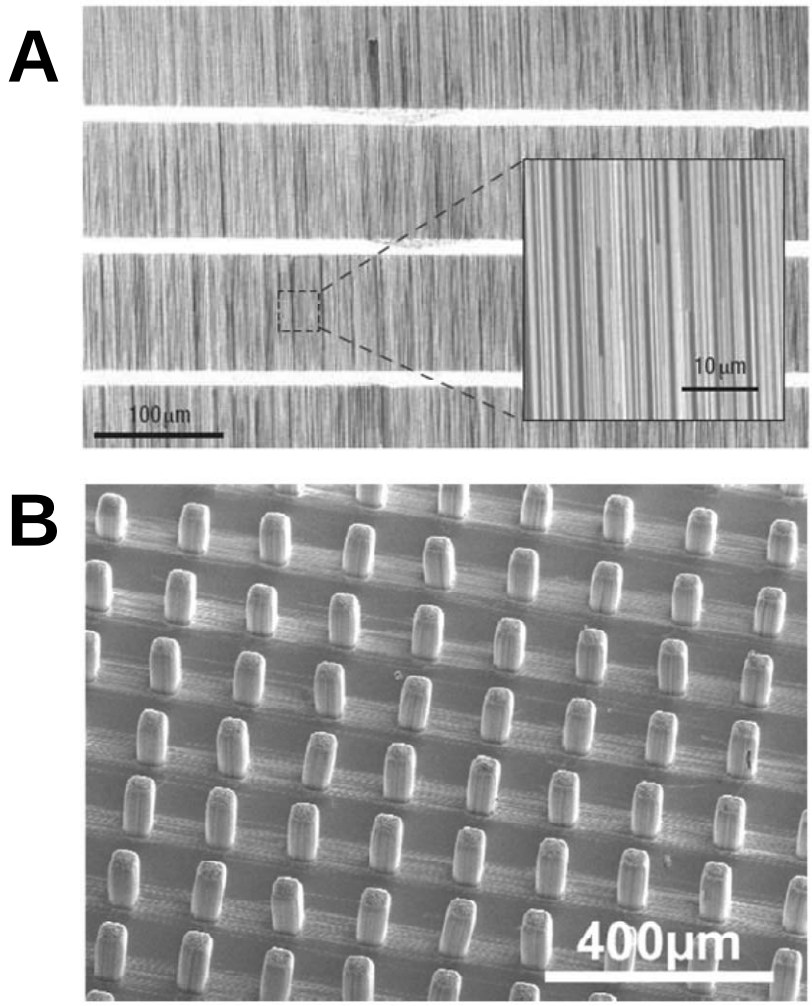

Figure 1. (A) SEM image of a pattern of perfectly aligned, perfectly linear SWCNTs formed by CVD growth on a quartz substrate. The bright horizontal stripes correspond to the regions of iron catalysts patterned by photolithography. Inset: a magnified SEM image. These arrays contain ~5 SWCNTs μm^{-1}. Reproduced with permission from Ref. [12]. Copyright 2007, Nature Publishing Group. (B) SEM image of 3D CNT architectures on quartz wafers by an orthogonally directed CVD growth. The vertical pillar forests are FWCNTs and the horizontal tubes are SWCNTs. Reproduced with permission from Ref. [18]. Copyright 2009, American Chemical Society.

Even though the multiple growth process is attractive but is trivial. Liu *et al.* has realized the growth of high-density parallel arrays of SWCNTs on ST-cut quartz substrates by using Cu as catalysts instead of Fe.[19] When Cu line patterns are used as catalysts, the density can reach >50 SWCNT μm^{-1} even without thermal annealing quartz substrate. In detail, the patterned substrate

was treated with O_2 plasma for 15 min, followed by CVD growth of SWCNTs at 900 °C with a flow of H_2 (400 sccm) and Ar (150 sccm, through an ethanol bubbler). Importantly, direct proof of "tip growth" mechanism and direct evidence that explained the termination of SWCNT growth were demonstrated. For example, the authors have observed the formation of "sickle" shaped nanotubes when using spin-cast nanoparticles as catalysts. The increase in the size of catalyst nanoparticles as a result of merging with unreacted nanoparticles on the substrate is believed to be the cause of bending and termination of nanotubes. It is expected that the SWCNT arrays with such high density will find immediate applications in transistors and other classes of electronic devices, such as analog radio frequency electronics.[20]

The patterning of catalysts by aforementioned conventional photolithography normally involves two major steps, *i.e.* patterning of photoresist and coating of catalysts (*e.g.* spin-casting of Fe iron solution or e-beam evaporation of Fe). In order to shorten the processing time, one step approach of patterning catalysts for the growth of dense, aligned parallel SWCNT arrays has been recently developed by Zhou and coworkers.[21] Simply, Shipley 1827 photoresist associated with $FeCl_3$ was spin-cast on ST-cut quartz wafers. Photolithography process and additional O_2 treatment will fabricate catalyst lines composed of iron oxide. Arrays of SWCNTs with perfect alignment and very uniform density of ~10 SWCNT μm^{-1} were obtained by CVD performed at 920 °C with a flow of CH_4/H_2 gas mixture (1100 sccm/220 sccm). The length of most SWCNTs exceeds 200 μm. They aligned perfectly along the crystallographic direction except some short curved tubes are found at the catalyst regions. It is noted that the thermal treatment of quartz wafers at high temperature (900 °C in air for 1 h) is needed before photolithography since high temperature will decrease surface –OH group quantity and thus improve the adhesion between photoresist and quartz wafers. Furthermore, the photoresist polymer plays a prominent role in the

formation of mono-dispersed nanoparticles for the growth of SWCNTs in CVD. First, the polymer can effectively prevent the formation of large particles during drying at room temperature and then heating at 700 °C. Second, the polymer layer can help the substrates anchor the catalyst nanoparticles. Zhou *et al.* recently applied this one-step approach to patterning catalyst islands on Y-cut quartz wafers from which the orthogonal growth of vertical few-walled carbon nanotubes (FWCNTs) forests and horizontal SWCNT arrays were demonstrated.[18] $FeCl_3$ was mixed with Shipley 1813 positive photoresist as the catalyst precursor. The growth of vertically aligned FWCNTs or horizontally aligned SWCNTs can be selectively achieved by delicately controlling CVD conditions. For example, in order to grow FWCNTs, CVD was operated at 850 °C with a gas flow of C_2H_4 (90 sccm: standard cubic centimeters per minute) and H_2 (200 sccm) together with an Ar/water vapor mixture (800 sccm); whereas SWCNTs can be subsequently grown at 900 °C with a gas flow of hydrogen (750 sccm) and argon (600 sccm, through a methanol bubbler, and 150 sccm, through an ethanol bubbler). As such, a 3D hierarchical nanotube structure composed of vertical FWCNT forests and horizontal SWCNT arrays was obtained, Figure 1B. Importantly, the FWCNT forests can be used as electrodes instead of metal contacts. This will avoid problems in the fabrication of metal contacts, such as large contact resistance from Schottky barrier[6] and contamination from photoresist remnants. The SWCNTs play the role of conducting channels. Field-effect transistors based on this 3D architecture have been demonstrated. It is worthwhile noting that in comparison to silicon and sapphire wafers, quartz substrate shows a superior role for the orthogonal nanotube growth. Meanwhile, a “base-growth” mechanism is found to be responsible for the growth of FWCNT forest.

Besides these conventional photolithographic techniques, a few reports have used synchrotron-radiation lithography to prepare patterned Si or SiO_2 substrates (pillars and lines). Thin film of Fe or Co was deposited on these patterned substrates for SWCNT growth.[22, 23] Suspended networks of SWCNTs which bridge the patterned pillars or lines were obtained after CVD growth. These methods demonstrate that the assembled SWCNT networks can grow on nanostructured substrates and show promises for the self-assembly of interconnections which is important for nanoelectronics. Photolithography has thus proved to be successful for patterning catalysts, but it also suffers from some limitations, such as requirement of sophisticated equipments and multiple-step processes. Moreover, patterning catalyst at the single-particle level at specific locations for growth of SWCNT arrays is a challenging task for photolithography. More facile methods to patterning catalysts should be developed.

2.2 Contact printing

Microcontact printing (μCP) has been proven a suitable microfabrication tool for patterning small molecules, biomolecules and nanomaterials on micrometer scale over large surface area. In brief, the patterned stamps (commonly poly(dimethylsiloxane), PDMS) with raised and recessed features (Figure 2A) were coated with materials of interest and then were brought in contact with substrates and transfer materials onto substrates. As such, the patterns were formed. Most importantly, the low cost and easy fabrication of stamps and easy operation of printing process renders μCP widely accessible. It is thus desirable to print catalyst nanoparticles on wafers directly by μCP for the growth of SWCNTs. Li *et al.* had demonstrated the printing of Fe_2O_3 nanoparticle lines by μCP for growth of SWCNTs.[24] In their experiment, $FeCl_3$ ethanol solution

was first coated on an as-prepared PDMS stamp with line or dot features. During the ink drying process, $Fe_2O_3 \cdot \chi H_2O$ nanoparticles were formed on the stamps from the hydrolysis of $FeCl_3$. The nanoparticles were then transferred onto the Si/SiO_2 substrate to form patterns, Figure 2A. The diameter of as-formed nanoparticles and their populations in the patterns can be adjusted by changing the concentration of the applied $FeCl_3$ ethanol solution. For example, $Fe_2O_3 \cdot \chi H_2O$ nanoparticles with a mean size of ~20 nm were formed when the ink concentration was 0.2 mM. It was further found that at higher concentrations, ink will aggregate at the pattern edges and thus it is suggested to use lower ink concentration for the generation of nanoparticles. Using the Fe_2O_3 nanoparticles as catalysts, networks of SWCNTs with high density were yielded after thermal CVD growth, Figure 2B. CVD was performed at 900 °C with CH_4 (800 sccm) as the feeding gas for 15 min. Notably, very few SWCNTs grew on the patterns if high ink concentration was used since large particles were formed which do not favor the growth of SWCNTs. The authors had extended this method to pattern other metal oxides, *e.g.* Ni-containing particles. In addition, the direct patterning of ferritin for the growth of multi-walled CNTs (MWCNTs) has been reported by Bonard *et al.*[25]

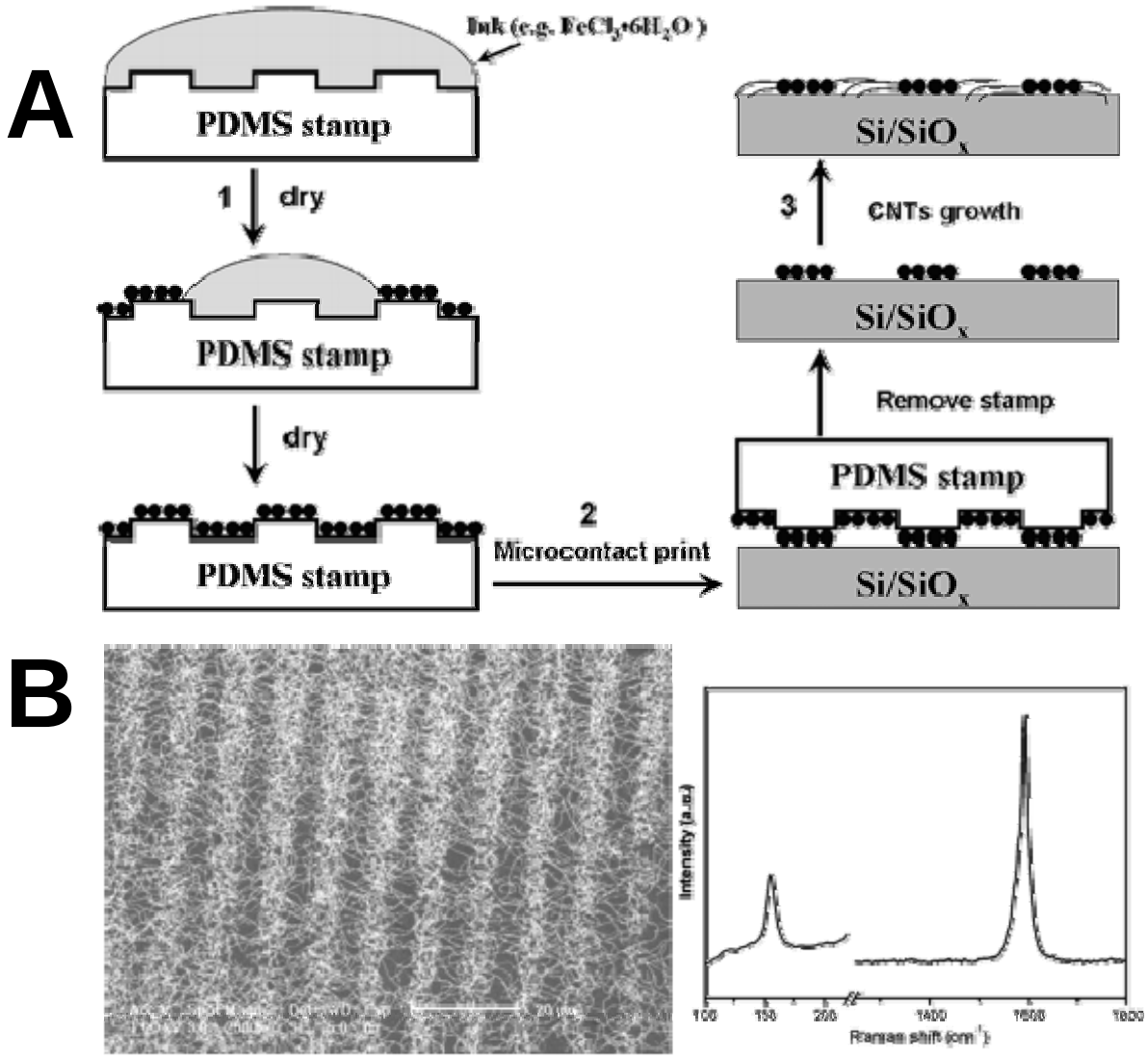

Figure 2. (A) Printing of catalyst inks (Step 1: Ink the stamp with $FeCl_3 \cdot 6H_2O$ ethanol solution; Step 2: Bring the inked stamp in contact with substrate and transfer $Fe_2O_3 \cdot \chi H_2O$ nanoparticles) and CVD growth of SWCNTs (Step 3). (B) SEM image and Raman characterization of SWCNTs grown from the fabricated $Fe_2O_3 \cdot \chi H_2O$ nanoparticles on the Si/SiO_2 surface by CVD. 1.0 mM $FeCl_3 \cdot 6H_2O$ ethanol solution was used as the ink for μCP, scale bar = 20 μm. Reproduced with permission from Ref. [24]. Copyright 2006, American Chemical Society.

Besides the direct print of the iron salts by μCP, Zhou *et al.* reported the patterning of a mixed ink of $FeCl_3$ and polyvinylpyrrolidone (PVP) as catalyst precursors for the growth of perfectly aligned SWCNT arrays.[21] The association of $FeCl_3$ with polymers increases the reproducibility of μCP process. In the meantime, the introduction of polymers renders the control of particle size

easier and prevents the formation of large particles during drying of the mixture. For example, when 40 mmol L^{-1} PVP solution was applied, high density particles with a diameter of less than 1 nm were obtained. This delicate control of particle size may prove useful for the growth of SWCNTs even though the reported results show no apparent relationship between size and density of nanoparticles and quality of arrays of SWCNTs they generated. Instead of Si/SiO_2 substrates, quartz wafers were used. Higher density of perfectly aligned SWCNTs along the underlying crystallographic direction was thus achieved.

Instead of using pre-patterned PDMS stamps, Dai *et al.* used flat PDMS stamps to transfer catalysts onto a patterned silicon substrate with regular pillars.[26] The used catalyst precursor was a mixture of three general components which are inorganic chloride ($AlCl_3 \cdot 6H_2O$, $SiCl_4$, $FeCl_3 \cdot 6H_2O$ and MoO_2Cl_2), a removable triblock copolymer (*i.e.* P103 or P-123 poly(alkylene oxide)) serving as the structure-directing agent for chlorides, and appropriate alcohol (BuOH, EtOH, or MeOH) for dissolution of chloride and polymer. The as-prepared catalyst precursor was then spin-cast on a flat PDMS stamp which was pre-treated with oxygen plasma to render its surface hydrophilic. The inked-stamp was then placed on a patterned silicon substrate, leaving catalysts on the regular pillars. Subsequent calcination of the stamped substrate and CVD growth (900 °C, 750 mL min^{-1} methane flow for 20 min) resulted in the growth of SWCNTs arrays. Interestingly, it was found that the SWCNTs grew with delicate directionality, *i.e.* they bridged and suspended between the isolated silicon pillars. This directionality of the suspended tubes arises from the designed substrate. The CNTs which grew to adjacent pillar suspended and flew under the support of the methane flow, whereas other tubes which grew towards other directions fell into the side walls of the pillars. This study paves the way for the growth of suspended SWCNT networks and also opens the possibility of probing the intrinsic property of SWCNTs,

e.g. electrical property, without the interference of underlying substrate. The study of mechanical property, *e.g.* tensile strength, becomes feasible without etching substrates. By using the catalyst precursors with similar formulation, Gu *et al.* printed catalysts onto thin Si_3N_4 membranes with the pre-patterned stamp, which were used for the growth of SWCNT networks.[27]

Although the contact printing method proves desirable for printing catalyst used for growth of SWCNTs in terms of low cost, easy access and high throughput, similar to photolithography, the achieved catalyst pattern is normally micrometer in size, rendering it incapable for growing SWCNT arrays at the single-tube level. Therefore, methods that can pattern catalyst at much better resolution or even single-particle level are required.

2.3 E-beam lithography and focused ion beam lithography

Electron-beam lithography (EBL) uses electron beams to scan a surface covered with resist film and patterns are formed after the lift-off process. It has many advantages in patterning surfaces, such as the capability to pattern at precise locations, with defined shapes and substantially small sizes (*e.g.* 5 nm), which are not achievable with photolithography or μCP. EBL has been widely applied to pattern catalysts for the growth of SWCNTs. Dai *et al.* have achieved the synthesis of individual SWCNTs from EBL-generated catalyst patterns on SiO_2 substrate.[28] Briefly, EBL was used to pattern squares of various sizes with different spacing on PMMA thin film-coated SiO_2 substrate. After removal of the exposed PMMA with solvents, squares of 3 or 5 μm with a spacing of 10 μm were generated, for example. Drop-casting of $Fe(NO_3)_3 \cdot 9H_2O$, $MoO_2(acac)_2$ and alumina nanoparticles generated the catalyst patterns after baking the substrate at 170 °C and the lift-off of the remaining PMMA. CVD growth with controlled experimental conditions

(methane, 1000 mL min^{-1} and 1000 °C) yielded high quality of SWCNTs, whose diameter mainly lies in the range of 1-3 nm. Several remarkable features can be observed from the growth of SWCNTs by this approach. First, 90% of the synthesized nanotubes are individual SWCNTs. Second, most nanotubes are straight, without any kinks forming, indicating that the tubes are free of topological defects and have high quality for electrical devices and fundamental studies. Third, many nanotubes are found to bridge and crosslink the microscopic catalyst patterns. Individual SWCNT electrical circuits have been fabricated and demonstrated based on thus bridging of nanotubes across catalyst patterns. In addition to the test of electrical properties, the authors have measured and estimated the tensile strength of SWCNTs (of the order of 200 GPa). This approach can be extended to pattern other catalysts other than Fe/Mo, such as Ni and Co. Importantly, with the ability to specifically locate the catalysts, the authors have provided direct evidence to support the "base-growth" mechanism of the SWCNTs, in which the growth end of SWCNTs remains free of catalysts.

Since the initial demonstration of EBL patterning catalysts for growth of SWCNTs, many improvements have been made. Most intriguingly, the Dai group recently reported the patterning of regular arrays of 2 nm metal nanoparticles on Si/SiO_2 by EBL for deterministic synthesis of nanomaterials, especially SWCNTs.[29] Figures 3A-B show the scheme of EBL patterning and particle formation from diffusion and clustering of metal atoms at elevated temperature on substrates. After lift-off of PMMA and thermal annealing, discrete clusters are formed in arrayed fashion. Since the diffusion length and quantity of metal atoms in the well largely determine the number and size of nanoparticles formed, it is critical to optimize the well size, annealing temperature (related to metal atom diffusion) and metal evaporation conditions in order to achieve individual nanoparticles with a narrow size distribution. For example, for Co

nanoparticles, the optimal annealing temperature for single particle formation in ~20 nm well is ~825 °C. Whereas the optimal annealing temperature for individual ≤5 nm Fe and Pt nanoparticles are ~775 and 900 °C, respectively. Figure 3C shows four SWCNTs grown on the individual Co nanoparticles. Importantly, the synthesized SWCNTs have monodisperse diameter. This opens possibilities for nanoelectronics since band gap is governed by the tube diameter. Further control over tube growth direction, *e.g.* patterning catalysts on substrates containing guiding lattices, and tube-tube distance will yield SWCNT arrays which are potential for high-performance electronics.

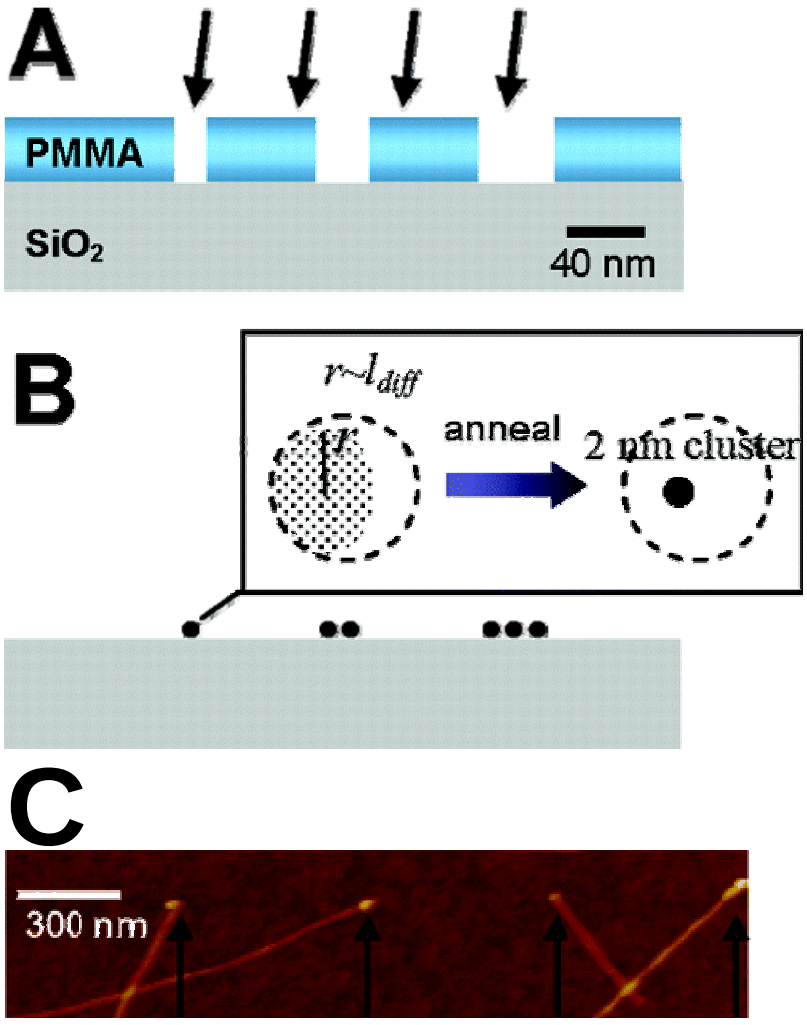

Figure 3. Formation of regular arrays of metal clusters down to 2 nm in diameter. (A) Arrays of 20-50 nm wells are patterned in ~100 nm thick PMMA on Si/SiO_2 (10 nm) substrates by EBL. Thin metal films (0.2-2 nm) are then deposited by an electron-beam evaporator at a 5-10° angle with respect to the substrate normal. (B) After lift-off and annealing, one or multiple particles per well are formed depending on the well size. An individual nanoparticle of ~2 nm is shown in the inset. (C) AFM images of four SWCNTs grown from individual nanoparticles. The mean diameter of SWCNTs is ~1.7 nm. Reproduced with permission from Ref. [29]. Copyright 2005, American Chemical Society.

Analogous to EBL, focused ion beam lithography (FIB) uses high-energy ion beams instead of electron beams to pattern surfaces. Peng *et al.* had reported the generation of Fe catalyst patterns by FIB for patterned growth of SWCNT arrays.[30] In their report, ordered arrays of SWCNTs were grown by thermal CVD from patterned Fe catalysts on a variety of substrates, including Si, SiO_2, Al_2O_3 and Si_3N_4. Specifically, the introduction of external electric fields proved effective to control the orientation of SWCNTs during CVD growth compared with the guiding forces of nanotube-substrate and nanotube-nanotube interactions and thermal vibrations. This growth strategy provides an alternative approach for growth of SWCNTs from catalyst patterns with controlled locations and nanometer size.

In addition, both EBL and FIB can in principle be used to pattern resist films mixed with catalyst salts (see Section 2.1), so that one step process can generate catalyst patterns for growth of SWCNTs. Importantly, these maskless, direct-patterning lithographic techniques show advantages for depositing catalysts at specific locations for growth of SWCNTs, which is helpful for their integration to electronic devices. However, it is worth noting that these methods suffer from the low throughput, making them unsuitable for large-area patterning of catalyst and thus growth of wafer-scale SWCNT arrays.

2.4 Dip-pen nanolithography

Invented in 1999, dip-pen nanolithography (DPN)[31, 32] is a direct-write and non-destructive scanning probe microscopy-based lithography (SPL), which employs an ink-coated atomic force microscopy (AFM) tip to directly deposit molecules onto substrates of interest to form patterns. DPN is capable of generating micro- and sub-100 nanometer patterns for almost any kind of materials. More importantly, this technique allows the deposition of materials at precise locations, which can be useful for device fabrication. Thus, it is easily envisioned to pattern catalysts on substrates by DPN and grow SWCNTs at precisely controlled locations. Recently, our group has reported the deposition of Co nanoparticles by DPN on both SiO_2 and quartz substrates for growth of SWCNT arrays.[33] The DPN process is schematically shown in Figure 4A. Briefly, a "scanning-coating" strategy was developed to effectively coat AFM tips with Co nanoparticles (NPs). After a small amount of Co NP solution was dropped on a Si/SiO_2 surface and then partially evaporated under ambient conditions, the AFM tip carefully touched the minidroplet of Co naniparticle solution and scanned for 1–2 min to coat the nanoparticles. DPN patterning was performed with thus ink-coated AFM tip, generating arrays of dot with a diameter as small as 68 nm. Meanwhile, most generated dot patterns have a thickness of ~11 nm, corresponding to 2-3 layers of Co nanoparticles. Subsequent CVD process performed at 900 °C using ethanol as the feeding gas resulted in high quality SWCNTs, confirmed by AFM, SEM, and Raman spectroscopy. Remarkably, since DPN is capable of generating complex structures of catalysts, SWCNT networks of various complex patterns, *e.g.* letters or zigzag lines, were generated. In accordance with previous reports, when catalysts were patterned on SiO_2, SWCNTs grew along random direction and formed random SWCNT networks. Figure 4B shows a SEM image of arrayed SWCNT networks on SiO_2. However, the aligned SWCNT arrays can be generated if

quartz substrate was used. Importantly, this experiment provided direct evidence of the "base-growth" mechanism for SWCNTs. Furthermore, with the development of parallel pen DPN[34, 35] and polymer pen lithography,[36] the patterning of catalysts and growth of SWCNTs over wafer-scales is reliable. Kuljanishvili *et al.* used the similar strategy with multipen DPN to deposit iron-based catalysts for the growth of SWCNTs and fabricated a device based on the grown SWCNTs.[37] Worth commenting is that if the size of DPN-generated pattern can be controlled down to single particles, individual-tube arrays can be grown on quartz substrate, which is crucially important for individual-tube devices. By combining the recently developed scanning probe block copolymer lithography which can generate single-particle arrays,[38] such endeavor of generating individual-tube arrays is possible.

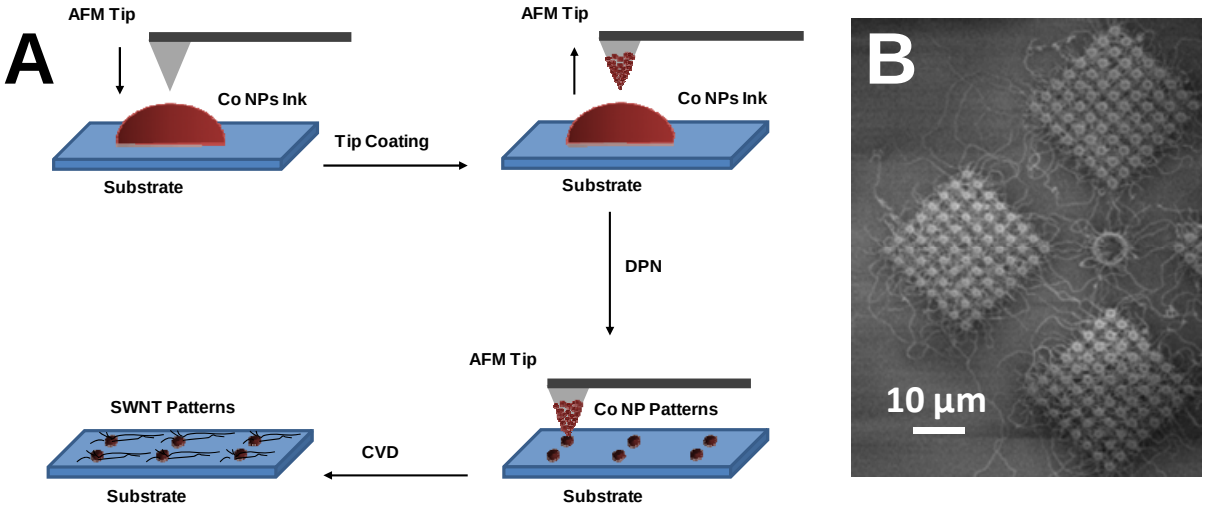

Figure 4. (A) Schematic illustration of the process: AFM tip coating, fabrication of Co NP patterns by DPN, and growth of SWCNTs on Co NP patterns. (B) SEM image of SWCNTs grown on the DPN-generated Co nanoparticle dot arrays on a SiO_2 substrate. Reproduced with permission from Ref. [33]. Copyright 2008, John Wiley & Sons, Inc.

Recently, a similar scanning probe microscopy-based approach has been reported to directly write catalysts for the growth of SWCNTs, in which glass nanopipettes filled with iron-based catalyst solutions were used instead of the ink-coated AFM tips. This method has advantages in terms of large reservoir of catalyst inks for long-time and large-area patterning.[39]

Besides the constructive DPN, it is worthwhile mentioning the destructive SPL, which uses scanning probe microscopy tips to mechanically or electrochemically damage surfaces and thus form patterns on substrates. Several studies report the patterning of catalysts by destructive SPL for the growth of MWCNTs but not SWCNTs,[40] but, in principle, the growth of SWCNTs from destructive SPL-generated catalyst patterns is possible.

2.5 "Scratching" methods

So far, all the methods described above to pattern catalysts for growth of aligned SWCNT arrays need either sophisticated equipments and/or complex procedures. It is therefore desirable to develop simple, cost-effective method to pattern catalysts which can subsequently be used to grow SWCNTs. Our group has recently reported a "needle-scratching" method (NSM) to achieve fast catalyst patterning used for large-scale growth of densely aligned SWCNT arrays.[41] Figure 5A schematically shows the experimental setup. In brief, a common syringe needle was controlled by a micromanipulator and scratched on a quartz or SiO_2 substrate. After that, CVD was performed to result in high quality and density SWCNTs,[33] which were confirmed by AFM, SEM and Raman spectroscopy. Interestingly, lots of nanoparticles were found in the scratched areas, which were used as catalysts for growth of SWCNTs. In addition to the random SWCNT networks grown on SiO_2, arrays of long, aligned SWCNTs were grown on quartz substrate when

strips of catalysts were fabricated by NSM (Figure 5B-C). The growth direction of SWCNTs matches the underlying substrate crystal lattice, following the [100] direction of quartz. Importantly, the density of the obtained SWCNTs can be as high as 10 tubes μm^{-1}, paving a way to growth high-density SWCNT arrays.

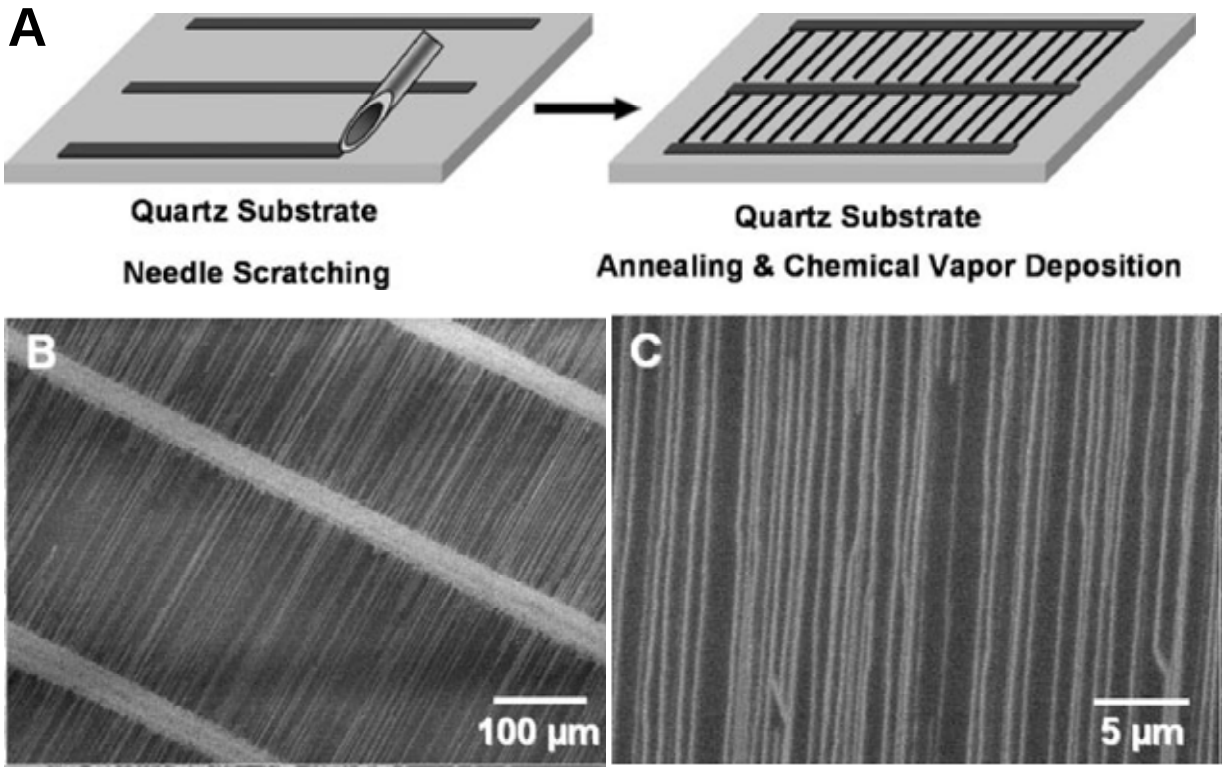

Figure 5. (A) Schematic illustration of the procedure for patterning catalyst stripes on substrates by NSM, which are used as catalysts for growth of dense, aligned SWCNTs by CVD. (B, C) SEM images of SWCNT arrays grown from needle-scratched catalyst stripes on quartz. Reproduced with permission from Ref. [41]. Copyright 2009, John Wiley & Sons, Inc.

In addition, this study also offers evidence on growth of SWCNTs from nonmetal catalysts. The elemental analysis proved that the "scratched" NPs were mostly nonmetal particles, demonstrating that in this study nonmetal particles, instead of metal particles, are responsible for growth of SWCNTs. This observation is in agreement with the recent reports that SiO_2 particles

can be used as catalysts to grow SWCNTs.[42, 43] Importantly, NSM is a simple but robust technique for patterning catalysts for growth of densely aligned SWCNT arrays. Many advantages can be found. Compared with photolithography or other lithographic techniques, NSM is simple and cost-effective. Moreover, NSM is a chemical-free and therefore environmentally friendly green approach. Worthwhile mentioning is that our group has extended this NSM to common metal objects such as blades and knives in addition to the syringe needles, further reducing the cost and improving its applicability.[44] Based on the "scratching" method, our group has fabricated "all-carbon" electric devices, *i.e.* single SWCNT and reduced graphene oxide films were used as channel material and electrodes, respectively.[45]

2.6 Other patterning methods

In addition to the aforementioned patterning methods, a few other methods are also worth brief mentioning. Note that the following methods may be used to grow MWCNTs or vertically aligned instead of horizontally aligned SWCNTs.

Ink-jet printing is a well-established printing technique, such as its use in printers and electronics printing. One major advantage is its high throughput. It has been used to pattern catalysts for site-selective growth of MWCNTs.[46] Further control of catalysts and CVD growth conditions will in principle allow the patterned growth of SWCNTs.

Nanosphere lithography (NSL) was initially developed to fabricate metal structures used for studying the localized surface plasmon resonance. In a typical NSL process, monodispersed spherical particles with size of micrometers or sub-micrometers are self-assembled on a surface to form a close-packed hexagonal structure, which is normally used as a mask for evaporation of

metals (*e.g.* Ag). As such, periodic metal nanostructures can form in the void areas between the particles after removal of particles using lift-off process. Zhou and coworkers used NSL to produce highly ordered catalyst nanoparticles (Fe, Ni or Co) with narrow size distribution.[47] Combining NSL and photolithography, highly aligned SWCNT arrays were obtained after CVD growth which was performed at 900 °C for 10 min under gas flows of CH_4 (2000 sccm), C_2H_4 (17 sccm) and H_2 (600 sccm). Raman spectroscopy showed that clean and defect-free nanotubes were grown.

Some methods, such as block copolymer lithography, can generate arrays of nanoparticles with monodispersity in size. Combined with the lithographic technique, *e.g.* photolithography, catalyst patterns can be easily achieved. Lu *et al.* demonstrated that high-quality SWCNTs with small diameter, controlled density and precise locations can be grown on the photolithography-patterned catalysts using a polyferrocenylsilane block copolymer catalyst precursor.[48]

3. Applications: an example

SWCNTs have received myriad applications, such as electronics, optoelectronics, composites, energy storages, medicine and sensors.[5] The application of the grown SWCNT arrays in high performance electronics has been demonstrated by Rogers and others.[12] Herein, an innovative application that uses aligned SWCNTs as polarization-sensitive, molecular near-field detectors is introduced.[49] This example highlights that besides the promising applications in nanoelectronics, many new and exciting applications based on aligned SWCNT arrays are waiting to be explored.

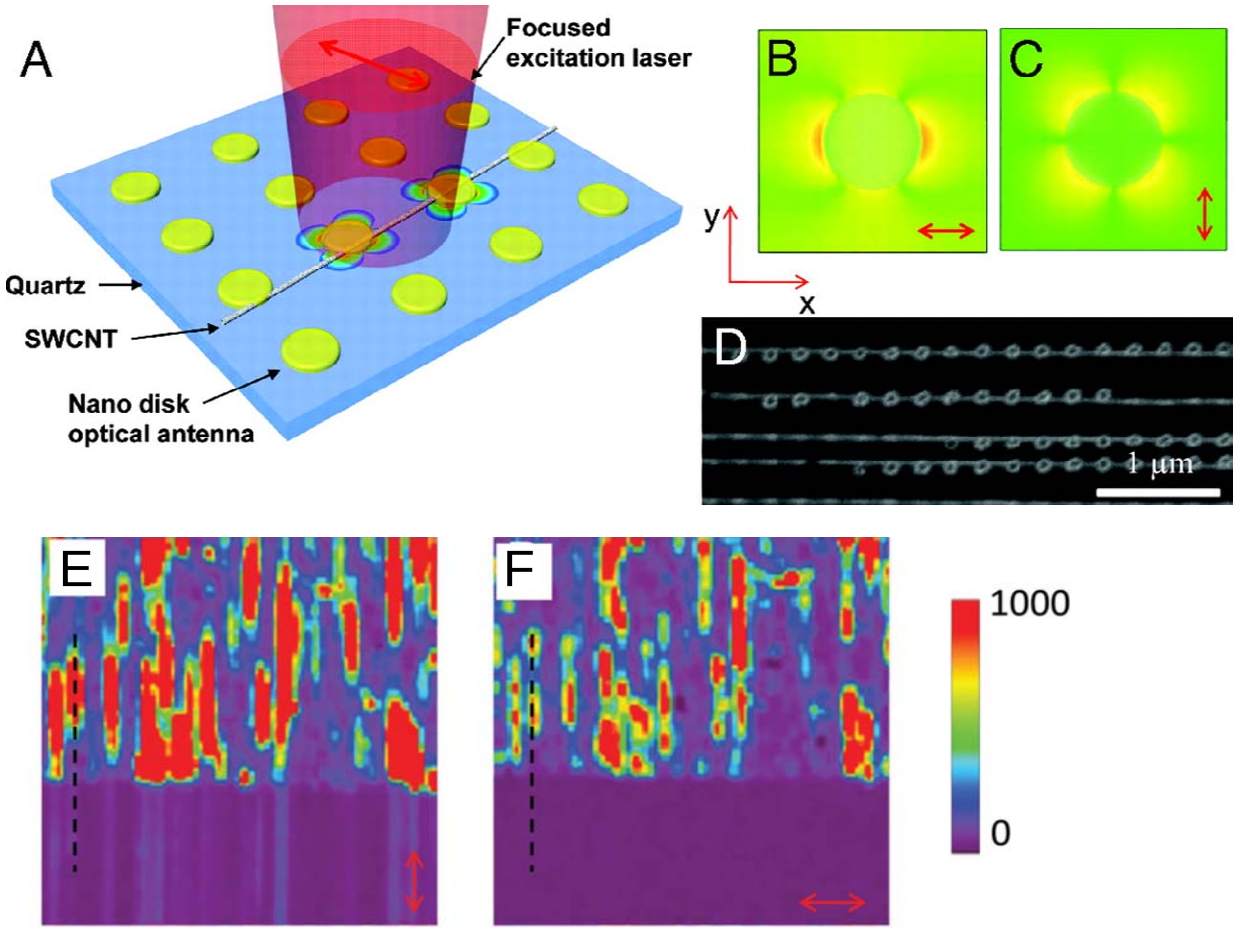

Figure 6. Schematic illustration of the polarization-sensitive SWCNT near-field detector configuration. (A) A schematic of the spatial distribution in the vicinity of the metallic nanodisks of the near-field amplitude along the x direction, when the laser is polarized normal to the SWCNT. (B and C) Calculated near-field amplitude distribution along the x direction generated around a single nanodisk optical antenna in a square array for illumination polarized parallel (B) and perpendicular (C) to the SWCNT assumed oriented along the x direction. The red arrow shows the polarization of the incident plane wave. (D) Exemplary SEM image of the coupled system of the aligned SWCNT antennas and the Au nanodisk antenna array. (E) Confocal Raman microscope (CRM) image of a 20 μm × 20 μm area with the laser polarization along the SWCNTs. This image is generated by spectrally integrating the intensity in the G-band for every pixel. G-band emission from SWCNTs that are not in contact with the gold nanodisks is visible for this polarization because of the ‘‘SWCNT antenna’’ effect. Surface enhanced Raman scattering is driven by the near-field distribution shown in B. (F) Same as C for perpendicular laser polarization. Reproduced with permission from Ref. [49]. Copyright 2009, The National Academy of Sciences of the USA.

The experiment setup is shown in Figure 6A. In brief, aligned SWCNT arrays were firstly grown on a single crystal quartz wafer which contained patterned catalysts generated by photolithography as described in Section 2.1. The obtained SWCNTs are 1.5 nm in diameter and 100 μm in length. Then squared arrays of Au nanodisks, which lie on top of the aligned SWCNTs, were fabricated by standard lithography (Figure 6A and D). The good alignment between the nanodisks and the SWCNTs is visible in Figure 6D. The combination of nanotubes and nanodisks constitutes a unique nanoantenna system, which functions in a unique receiver-transmitter relationship. The "receivers" are the Au nanodisks and the "transmitters" are the SWCNTs. The parameters of Au disk array are chosen such that the plasmonic resonance wavelength matches that of the exciting laser (*i.e.* 633 nm laser). When the laser scans the disks and excites resonant oscillations, well-defined electromagnetic modes with a complex field pattern can be set up. This local optical field can couple to the adjacent, well-aligned SWCNTs. The coupling is highly-directional, with the nanotubes responding to the local field of the nanodisks when the field is along the direction of the nanotube axis. The confocal Raman microscope images of nanodisk arrays with laser polarization along and perpendicular to the SWCNT aligned direction clearly show that surface enhanced Raman scattering of SWCNTs is driven by the near-field distributed along the SWCNT directions (Figure 6E-F). Thus, a polarization-dependent, near-field detector is fabricated based on the combination of aligned SWCNTs and arrayed Au nanodisks, which can detect subwavelength features in nanostructures and provide information on the nature and symmetry of nanoparticles. This work opens new horizons in nanophotonics and plasmonics. Most importantly, the novel use of SWCNTs in these nanoantennas opens up broader vista of how SWCNT arrays can be used in new devices.

4. Conclusions and outlooks

The growth of SWCNTs from controlled locations along certain directions in CVD is of paramount importance for their integration to nanoelectronics and other classes of devices. This review focuses on the controlled growth of horizontally aligned SWCNTs but not vertically aligned ones, which have also been reported.[50-52] In particular, the patterning of catalysts with controlled dimensions and locations is the crucial prerequisite for growth of SWCNT arrays. We have presented herein an overview of the most used lithographic techniques that can pattern catalysts, spanning from the traditional photolithography and e-beam lithography to the state-of-the-art dip pen nanolithography. Each method has its advantages and disadvantages. For example, photolithography is promising for large-scale patterning but lacks the capability of routinely generating sub-micrometer catalyst patterns at controlled locations. In addition, even without specific illustration, the density of SWCNTs grown from each method varies. For example, photolithography and "scratching" methods can yield high density SWCNT arrays whereas DPN yields relatively low density. Therefore, depending on the purpose of applications of as-grown SWCNTs, the choice of different patterning techniques is needed. In addition to the patterning methods, the judicious choice of catalysts, substrates and CVD experimental conditions are also of great importance.

To date, the chirality control of SWCNTs grown from the patterned catalysts has been a challenging task. This is understandable since the chirality of the grown SWCNTs depends on a variety of parameters, *e.g.* size and composition of catalyst particles, the CVD conditions, *etc.* Due to the complex nature of CVD conditions (*e.g.* feed gas and temperature) and catalysts (*e.g.* composition and size), this review has not intended to discuss in detail their influences on growth of SWCNTs. Even though, a few recent reports have shown promises in the control of chirality.

For example, Sankaran *et al.* have linked catalyst composition to chirality distributions of as-grown SWCNTs by tuning Ni_xFe_{1-x} nanoparticles.[53] Kato *et al.* demonstrated the narrow-chirality distributed SWCNT growth from nonmagnetic catalysts, *i.e.* Au, under controlled plasma-CVD conditions.[54] More interestingly, Ishigami *et al.* found that in addition to orientation control, crystal planes of substrates affects the diameter and chirality of SWCNTs.[55] Combining these insightful findings with the aforementioned patterning techniques, it is reasonable to expect that SWCNT networks or aligned arrays with controlled chirality can be grown from patterned catalysts. Thus, electronic devices with desirable electrical properties will be obtainable. Further research and development both theoretically and experimentally on growth of SWCNT arrays from patterned catalysts with defined chirality is urgently needed in the near future.

Acknowledgement

This work was supported by AcRF Tier 1 (RG 20/07) and AcRF Tier 2 (ARC 10/10, No. MOE2010-T2-1-060) from MOE, CRP (NRF-CRP2-2007-01) from NRF, A*STAR SERC Grants (No. 092 101 0064) from A*STAR, CREATE program (Nanomaterials for Energy and Water Management) from NRF, and the New Initiative Fund FY 2010 (M58120031) from NTU.

Reference

1 S. Iijima, *Nature*, 1991, **354**, 56.
2 R. Saito, G. Dresselhaus and M. S. Dresselhaus, *Physical properties of carbon nanotubes*, Imperial College Press, 1998.
3 S. Iijima and T. Ichihashi, *Nature*, 1993, **363**, 603.

4 A. Jorio, G. Dresselhaus and M. S. Dresselhaus, *Carbon Nanotubes: Advanced Topics in the Synthesis, Structure, Properties and Applications*, Spinger, 2008.
5 R. H. Baughman, A. A. Zakhidov and W. A. de Heer, *Science*, 2002, **297**, 787.
6 P. Avouris, Z. Chen and V. Perebeinos, *Nat. Nanotechnol.*, 2007, **2**, 605.
7 A. A. Odintsov, *Phys. Rev. Lett.*, 2000, **85**, 150.
8 Y. Yan, M. B. Chan-Park and Q. Zhang, *Small*, 2007, **3**, 24.
9 J. Liu, A. G. Rinzler, H. Dai, J. H. Hafner, R. K. Bradley, P. J. Boul, A. Lu, T. Iverson, K. Shelimov, C. B. Huffman, F. Rodriguez-Macias, Y.-S. Shon, T. R. Lee, D. T. Colbert and R. E. Smalley, *Science*, 1998, **280**, 1253.
10 V. C. Moore, M. S. Strano, E. H. Haroz, R. H. Hauge, R. E. Smalley, J. Schmidt and Y. Talmon, *Nano Lett.*, 2003, **3**, 1379.
11 J. Kong, N. R. Franklin, C. Zhou, M. G. Chapline, S. Peng, K. Cho and H. Dai, *Science*, 2000, **287**, 622.
12 S. J. Kang, C. Kocabas, T. Ozel, M. Shim, N. Pimparkar, M. A. Alam, S. V. Rotkin and J. A. Rogers, *Nat. Nanotechnol.*, 2007, **2**, 230.
13 N. R. Franklin, Y. Li, R. J. Chen, A. Javey and H. Dai, *Appl. Phys. Lett.*, 2001, **79**, 4571.
14 Z. Jin, H. Chu, J. Wang, J. Hong, W. Tan and Y. Li, *Nano Lett.*, 2007, **7**, 2073.
15 Y. Zhang, A. Chang, J. Cao, Q. Wang, W. Kim, Y. Li, N. Morris, E. Yenilmez, J. Kong and H. Dai, *Appl. Phys. Lett.*, 2001, **79**, 3155.
16 P. G. Collins, M. S. Arnold and P. Avouris, *Science*, 2001, **292**, 706.
17 S. W. Hong, T. Banks and J. A. Rogers, *Adv. Mater.*, 2010, **22**, 1826.
18 W. Zhou, L. Ding, S. Yang and J. Liu, *J. Am. Chem. Soc.*, 2009, **132**, 336.
19 L. Ding, D. Yuan and J. Liu, *J. Am. Chem. Soc.*, 2008, **130**, 5428.
20 Q. Cao and J. Rogers, *Nano Res.*, 2008, **1**, 259.
21 W. Zhou, C. Rutherglen and P. Burke, *Nano Res.*, 2008, **1**, 158.
22 Y. Homma, Y. Kobayashi, T. Ogino and T. Yamashita, *Appl. Phys. Lett.*, 2002, **81**, 2261.
23 Y. J. Jung, Y. Homma, T. Ogino, Y. Kobayashi, D. Takagi, B. Wei, R. Vajtai and P. M. Ajayan, *J. Phys. Chem. B*, 2003, **107**, 6859.
24 L. Ding, W. Zhou, H. Chu, Z. Jin, Y. Zhang and Y. Li, *Chem. Mater.*, 2006, **18**, 4109.
25 J.-M. Bonard, P. Chauvin and C. Klinke, *Nano Lett.*, 2002, **2**, 665.
26 A. M. Cassell, N. R. Franklin, T. W. Tombler, E. M. Chan, J. Han and H. Dai, *J. Am. Chem. Soc.*, 1999, **121**, 7975.
27 G. Gu, G. Philipp, X. Wu, M. Burghard, A. M. Bittner and S. Roth, *Adv. Funct. Mater.*, 2001, **11**, 295.
28 J. Kong, H. T. Soh, A. M. Cassell, C. F. Quate and H. Dai, *Nature*, 1998, **395**, 878.
29 A. Javey and H. Dai, *J. Am. Chem. Soc.*, 2005, **127**, 11942.
30 H. B. Peng, T. G. Ristroph, G. M. Schurmann, G. M. King, J. Yoon, V. Narayanamurti and J. A. Golovchenko, *Appl. Phys. Lett.*, 2003, **83**, 4238.
31 R. D. Piner, J. Zhu, F. Xu, S. Hong and C. A. Mirkin, *Science*, 1999, **283**, 661.
32 D. S. Ginger, H. Zhang and C. A. Mirkin, *Angew. Chem. Int. Ed.*, 2004, **43**, 30.
33 B. Li, C. F. Goh, X. Zhou, G. Lu, H. Tantang, Y. Chen, C. Xue, F. Y. C. Boey and H. Zhang, *Adv. Mater.*, 2008, **20**, 4873.
34 H. Zhang, N. A. Amro, S. Disawal, R. Elghanian, R. Shile and J. Fragala, *Small*, 2007, **3**, 81.
35 K. Salaita, Y. Wang, J. Fragala, R. A. Vega, C. Liu and C. A. Mirkin, *Angew. Chem. Int. Ed.*, 2006, **45**, 7220.
36 F. Huo, Z. Zheng, G. Zheng, L. R. Giam, H. Zhang and C. A. Mirkin, *Science*, 2008, **321**, 1658.
37 I. Kuljanishvili, D. A. Dikin, S. Rozhok, S. Mayle and V. Chandrasekhar, *Small*, 2009, **5**, 2523.
38 J. Chai, F. Huo, Z. Zheng, L. R. Giam, W. Shim and C. A. Mirkin, *Proc. Natl. Acad. Sci. U. S. A.*, 2010, **107**, 20202.
39 B. Omrane and C. Papadopoulos, *IEEETrans. Nanotechnol.*, 2010, **9**, 375.
40 C.-C. Chiu, M. Yoshimura and K. Ueda, *Diamond Relat. Mater.*, 2008, **18**, 355.

41 B. Li, X. Cao, X. Huang, G. Lu, Y. Huang, C. F. Goh, F. Y. C. Boey and H. Zhang, *Small*, 2009, **5**, 2061.
42 B. Liu, W. Ren, L. Gao, S. Li, S. Pei, C. Liu, C. Jiang and H.-M. Cheng, *J. Am. Chem. Soc.*, 2009, **131**, 2082.
43 S. Huang, Q. Cai, J. Chen, Y. Qian and L. Zhang, *J. Am. Chem. Soc.*, 2009, **131**, 2094.
44 X. Cao, B. Li, Y. Huang, F. Boey, T. Yu, Z. Shen and H. Zhang, *ACS Appl. Mater. Interfaces*, 2009, **1**, 1873.
45 B. Li, X. Cao, H. G. Ong, J. W. Cheah, X. Zhou, Z. Yin, H. Li, J. Wang, F. Boey, W. Huang and H. Zhang, *Adv. Mater.*, 2010, **22**, 3058.
46 H. Ago, K. Murata, M. Yumura, J. Yotani and S. Uemura, *Appl. Phys. Lett.*, 2003, **82**, 811.
47 K. Ryu, A. Badmaev, L. Gomez, F. Ishikawa, B. Lei and C. Zhou, *J. Am. Chem. Soc.*, 2007, **129**, 10104.
48 J. Q. Lu, T. E. Kopley, N. Moll, D. Roitman, D. Chamberlin, Q. Fu, J. Liu, T. P. Russell, D. A. Rider and I. Manners, *Chem. Mater.*, 2005, **17**, 2227.
49 E. Cubukcu, F. Degirmenci, C. Kocabas, M. A. Zimmler, J. A. Rogers and F. Capasso, *Proc. Natl. Acad. Sci. U. S. A.*, 2009, **106**, 2495.
50 K. Hata, D. N. Futaba, K. Mizuno, T. Namai, M. Yumura and S. Iijima, *Science*, 2004, **306**, 1362.
51 L. Qu, F. Du and L. Dai, *Nano Lett.*, 2008, **8**, 2682.
52 L. Qu and L. Dai, *J. Mater. Chem.*, 2007, **17**, 3401.
53 W.-H. Chiang and R. Mohan Sankaran, *Nat. Mater.*, 2009, **8**, 882.
54 Z. Ghorannevis, T. Kato, T. Kaneko and R. Hatakeyama, *J. Am. Chem. Soc.*, 2010, **132**, 9570.
55 N. Ishigami, H. Ago, K. Imamoto, M. Tsuji, K. Iakoubovskii and N. Minami, *J. Am. Chem. Soc.*, 2008, **130**, 9918.

Table of Contents

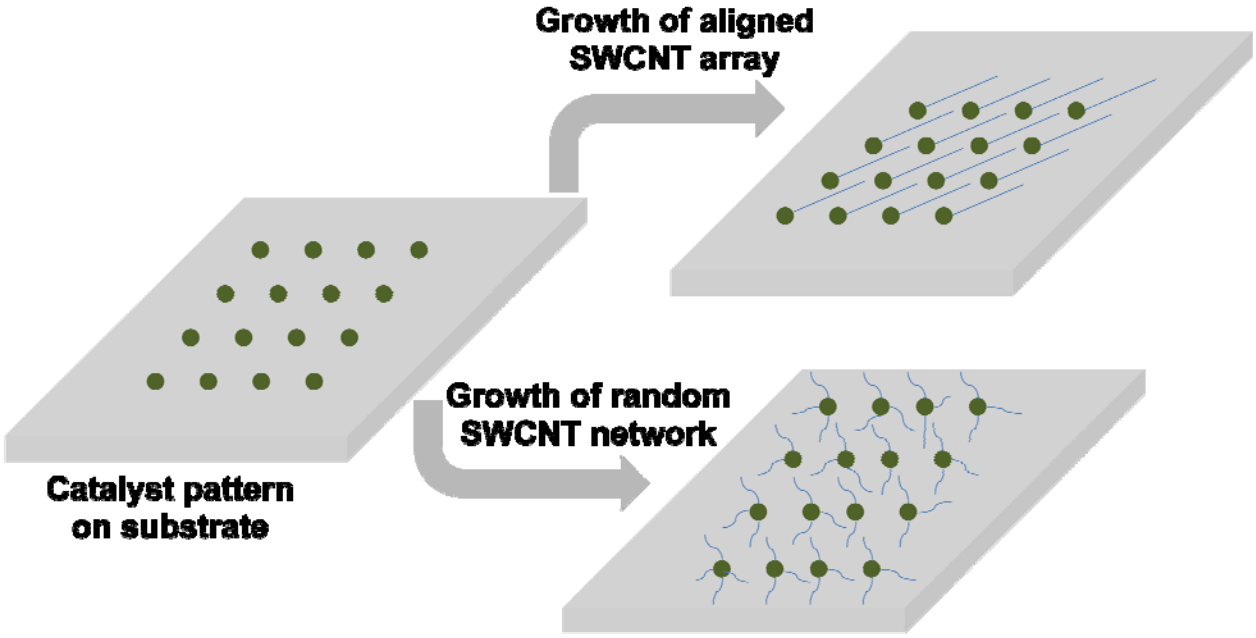

This review introduces the most commonly-used lithographic techniques to pattern catalyst on substrates for growth of single-walled carbon nanotubes.